Structural basis of a ribozyme's thermostability: P1–L9 interdomain interaction in RNase P RNA

MICHAL MARSZALKOWSKI, DAGMAR K. WILLKOMM, and ROLAND K. HARTMANN
Institut für Pharmazeutische Chemie, Philipps-Universität Marburg, D-35037 Marburg, Germany

ABSTRACT

For stability, many catalytic RNAs rely on long-range tertiary interactions, the precise role of each often being unclear. Here we demonstrate that one of the three interdomain architectural struts of RNase P RNA (P RNA) is the key to activity at higher temperatures: disrupting the P1–L9 helix–tetraloop interaction in P RNA of the thermophile *Thermus thermophilus* decreased activity at high temperatures in the RNA-alone reaction and at low Mg^{2+} concentrations in the holoenzyme reaction. Conversely, implanting the P1–P9 module of *T. thermophilus* in the P RNA from the mesophile *Escherichia coli* converted the latter RNA into a thermostable one. Moreover, replacing the *E. coli* P1–P9 elements with a pseudoknot module that mediates the homologous interaction in *Mycoplasma* P RNAs not only conferred thermostability upon *E. coli* P RNA but also increased its maximum turnover rate at 55°C to the highest yet described for a P RNA ribozyme.

Keywords: bacterial RNase P RNA; P1–L9 interdomain contact; thermostability

INTRODUCTION

The ribonucleoprotein enzyme RNase P catalyzes tRNA 5′-end maturation in all organisms and organelles (Schön 1999). In bacteria, the RNA subunit (P RNA), ~380 nucleotides (nt) in size and encoded by the *rnpB* gene, forms a specific complex with a single protein cofactor of ~13 kDa. In vitro, bacterial P RNA has robust catalytic activity in the absence of the protein (Guerrier-Takada et al. 1983), but the latter is essential for function in vivo (Schedl et al. 1974; Gößringer et al. 2006). P RNAs from bacteria are subdivided into two distinct structural groups, termed type A (for "ancestral") and type B (for "*Bacillus*"; Hall and Brown 2001). P RNAs of both types consist of two independent folding domains, the specificity (S-) and the catalytic (C-) domains (Loria and Pan 1996, 1997), which are oriented toward each other by three interdomain loop–helix contacts (Fig. 1A, L18–P8, L8–P4, P1–L9) in P RNAs of type A architecture. These long-range interactions, considered as architectural struts that stabilize the RNA's overall conformation, were originally identified by phylogenetic covariation analyses (Brown et al. 1996; Massire et al. 1997, 1998) and later confirmed in the crystal structure of P RNA from *Thermotoga maritima* (Torres-Larios et al. 2005). The importance of the aforementioned as well as other (intradomain) long-range tertiary interactions for P RNA function were also demonstrated experimentally (e.g., Darr et al. 1992; Pomeranz Krummel and Altman 1999). However, the specific functional contributions of the L18–P8, L8–P4, and P1–L9 contacts are poorly understood.

We recently reported that P RNAs from thermophilic bacteria share a 5′-GYAA L9 tetraloop and a P1 receptor site consisting of a G-C base-pair (bp) tandem, a combination not present in other bacteria (Marszalkowski et al. 2006). Also, helices P1 and P9 are stabilized in P RNAs from thermophiles by helix extension and/or deletion of nucleotide bulges. These observations prompted us to scrutinize the importance of the P1–L9 interaction in P RNA of the thermophile *Thermus thermophilus*, an A-type P RNA with robust in vitro activity at temperatures of up to 75°C (Hartmann and Erdmann 1991) and to compare it to that of the mesophile *Escherichia coli*.

RESULTS AND DISCUSSION

Activity of *T. thermophilus* P RNA with a disrupted P1–L9 interaction

Initially, we disrupted the P1–L9 interaction in *T. thermophilus* P RNA by a sequence change of the L9 loop (Fig. 1B,

Reprint requests to: Dagmar K. Willkomm, Institut für Pharmazeutische Chemie, Philipps-Universität Marburg, Marbacher Weg 6, D-35037 Marburg, Germany; e-mail: willkomm@staff.uni-marburg.de; or Roland K. Hartmann, Institut für Pharmazeutische Chemie, Philipps-Universität Marburg, Marbacher Weg 6, D-35037 Marburg, Germany; e-mail: roland.hartmann@staff.uni-marburg.de; fax +49-6421-2825854.

Article published online ahead of print. Article and publication date are at http://www.rnajournal.org/cgi/doi/10.1261/rna.762508.

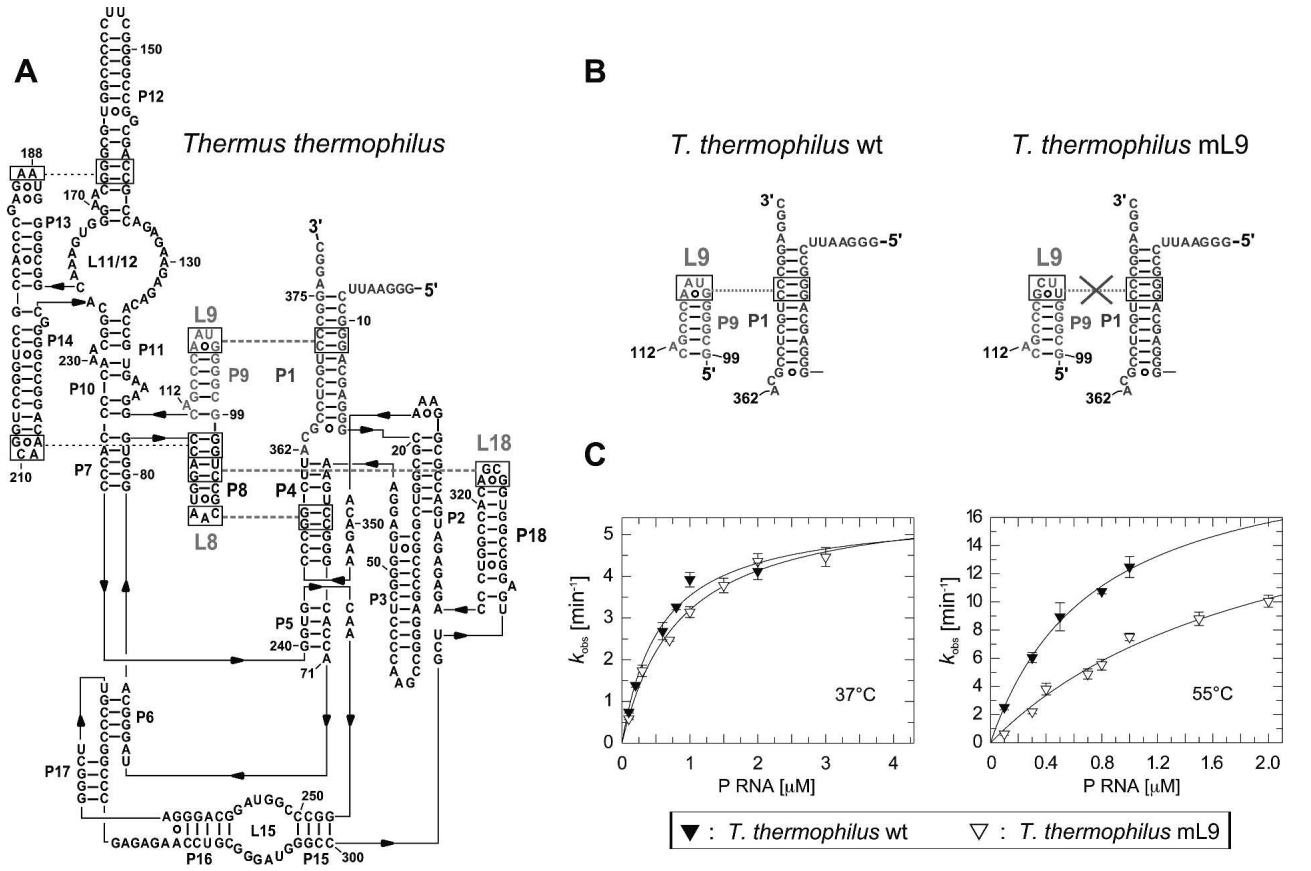

FIGURE 1. (*A*) Secondary structure presentation of *T. thermophilus* RNase P RNA according to Massire et al. (1998), with the three interdomain tetraloop–helix contacts L18–P8, L8–P4, and P1–L9 indicated by dashed lines. (*B*) P1–P9 region of the *T. thermophilus* wild-type P RNA (wt, *left*) and with the nucleotide exchanges in loop L9 that disrupt the P1–L9 interaction (mL9, *right*). (*C*) Processing assays with the two *T. thermophilus* P RNA variants. Assay conditions: 0.1–3 μM P RNA, <1 nM 5′-end labeled ptRNA, 100 mM $Mg(OAc)_2$, 100 mM NH_4OAc, 50 mM MES, and 2 mM EDTA (pH 6.0), and 37°C or 55°C as indicated. Error bars indicate standard deviations.

mL9, 5′-UUCG). At 100 mM Mg^{2+} in RNA-alone single turnover reactions, the mutant showed a defect at 55°C, but not at 37°C (Fig. 1C). This was caused mainly by a two- to threefold increase in $K_{m(sto)}$ ($K_{m(sto)}$, the single turnover K_m, describes the enzyme concentration at which the half maximum rate under conditions of [E] >> [S] is achieved) (Table 1). An even more pronounced defect (up to 24-fold decrease in cleavage rate) was seen in activity assays with reconstituted RNase P holoenzymes at 37°C and 2.0 or 4.5 mM Mg^{2+} (Table 2).

Role of the P1–L9 interaction in folding of *T. thermophilus* P RNA

Effects of the L9 mutation on P RNA folding were analyzed by native PAGE (Buck et al. 2005). While two main conformers were observed for *T. thermophilus* wild-type (wt) P RNA (Fig. 2A, bands 1,2), the L9 mutation indeed impeded formation of the faster migrating conformer 2, regardless of the presence or absence of P protein. To further characterize the two conformers of *T. thermophilus* wt P RNA, we eluted them separately from a native polyacrylamide gel at 4°C and reloaded aliquots of each eluate onto another native gel. Under these conditions, with the temperature not exceeding 15°C during elution and reelectrophoresis, both conformers did not reequilibrate to a substantial extent (Fig. 2B). In parallel, equal amounts of the two eluted conformers were tested in the holoenzyme reaction, performed at 22°C to mimize conformational reequilibration while maintaining high rates of substrate conversion. Approximately 15-fold higher activity (data not shown) was observed with the eluted conformer 2 (Fig. 2B, lane b) relative to eluted conformer 1 (Fig. 2B, lane a).

The catalytic deficits of the L9 mutant RNA observed at low metal ion concentration in the holoenzyme reaction thus appear to be directly correlated to a folding defect. Accordingly, the L9–P1 interaction is crucial for folding into a conformation that either stabilizes the catalytic core of the enzyme and its metal ion binding sites or has increased affinity for the P protein and/or the substrate.

TABLE 1. Summary of kinetic data of RNA-alone activity assays

	37°C		55°C	
RNase P RNA	$K_{m(sto)}$ (μM)	k_{react} (min^{-1})	$K_{m(sto)}$ (μM)	k_{react} (min^{-1})
T. thermophilus wt	0.56 ± 0.13	5.5 ± 0.5	0.85 ± 0.12	22.7 ± 1.8
T. thermophilus mL9	0.83 ± 0.12	5.8 ± 0.3	2.1 ± 0.5	20.9 ± 3.2
E.coli wt	0.65 ± 0.02	14.2 ± 0.1	1.3 ± 0.2	16.7 ± 1.5
E. coli mL9	0.33 ± 0.08	11.1 ± 0.8	0.9 ± 0.2	12.7 ± 1.2
E.coli P1P9 *Tth*	0.44 ± 0.09	11.4 ± 0.7	0.6 ± 0.1	25.2 ± 2.0
E.coli P1P9 *Mgen*	0.54 ± 0.15	10.9 ± 1.1	1.8 ± 0.2	35.1 ± 1.9
E.coli P1P9 *MgenA117C*	0.30 ± 0.08	10.4 ± 0.7	3.3 ± 0.7	58.6 ± 8.3
	$k_{react}/K_{m\ [37°]}$ ($min^{-1}\mu M^{-1}$)	$k_{react}/K_{m\ [55°]}$ ($min^{-1}\mu M^{-1}$)	$K_{react}/K_{m\ [55°]}$: $K_{react}/K_{m\ [37°]}$	
T. thermophilus wt	9.82	26.71	2.72	
T. thermophilus mL9	6.99	9.95	1.42	
E. coli wt	21.85	12.85	0.59	
E. coli mL9	33.64	14.11	0.42	
E. coli P1P9 *Tth*	25.91	42.00	1.62	
E. coli P1P9 *Mgen*	20.19	19.50	0.97	
E. coli P1P9 *MgenA117C*	34.67	17.76	0.51	

(wt) Wild type, ($K_{m(sto)}$) single turnover K_m (describes the enzyme concentration at which the half maximum rate under conditions of [E] >> [S] is achieved), (k_{react}) single turnover V_{max}. All quantifications are based on at least three independent experiments; errors are standard errors of the curve fit; for reaction conditions see Materials and Methods.

Role of the P1–L9 interaction in *E. coli* P RNA

We then investigated the role of the P1–L9 interaction in P RNA from the mesophile *E. coli* (Fig. 3A) by disrupting the P1–L9 interaction (Fig. 3B, *E. coli* mL9, 5′-UCCG mutation) as done previously (Pomeranz Krummel and Altman 1999). However, this neither substantially impaired the RNA-alone reaction at 37°C (in accordance with Pomeranz Krummel and Altman 1999) or 55°C nor the holoenzyme reaction (Fig. 3C; Tables 1, 2), thus contrasting our results for *T. thermophilus* P RNA. The mutation was further neutral to viability (Table 3): The *E. coli* L9 mutant *rnpB* gene provided on a low copy plasmid fully rescued growth of the *E. coli* P RNA mutant strain BW (Wegscheid and Hartmann 2006). Our data thus indicate that the P1–L9 interaction does not make a significant contribution to overall stabilization of *E. coli* P RNA. We like to note that an *E. coli rnpB* gene with the same L9 mutation failed to rescue the phenotype of *E. coli* strain NHY322 *rnpA49*, for which the temperature sensitivity of a mutant P protein at 43°C is compensated by P RNA overexpression (Pomeranz Krummel and Altman 1999). We do not know the reasons for this discrepancy, but the different nature of the test strains precludes a direct comparison.

Introduction of *T. thermophilus* and *Mycoplasma genitalium* P1–P9 elements into *E. coli* P RNA

We next replaced the P1–P9 elements of *E. coli* with those of *T. thermophilus* P RNA (Fig. 3B, *E. coli* P1P9 *Tth*).

TABLE 2. k_{obs} [min^{-1}] in RNase P holoenzyme assays of *T. thermophilus* and *E. coli* wild-type (wt) and mutant P RNAs

	E. coli P protein		*B. subtilis* P protein	
RNase P RNA	2 mM Mg^{2+}	4.5 mM Mg^{2+}	2 mM Mg^{2+}	4.5 mM Mg^{2+}
T. thermophilus wt	1.3 ± 0.2	4.0 ± 0. 4	1.1 ± 0.1	3.5 ± 0.4
T. thermophilus mL9	0.054 ± 0. 008	0.2 ± 0.02	0.28 ± 0.03	0.55 ± 0.02
E.coli wt	3.8 ± 0.4	3.8 ± 0.4	3.0 ± 0.3	4.0 ± 0.3
E. coli mL9	3.7 ± 0.5	4.2 ± 0.4	3.7 ± 0.4	4.1 ± 0.4
E.coli P1P9 *Mgen*	6.5 ± 0.5	8.4 ± 1.0		
E.coli P1P9 *MgenA117C*	3.2 ± 0.3	3.2 ± 0.3		

Reactions were performed as multiple turnover kinetics with recombinant P protein at 37°C in a buffer containing 20 mM HEPES, 150 mM NH_4OAc, 2 mM spermidine, 0.05 mM spermine, 4 mM β-mercaptoethanol (pH 7.4) at 37°C and 2 or 4.5 mM $Mg(OAc)_2$ as indicated, at concentrations of 10 nM P RNA, 100 nM substrate, and 40 nM P protein; k_{obs} is given as nanomoles substrate converted per nanomole of RNase P RNA per minute. For further details see Materials and Methods.

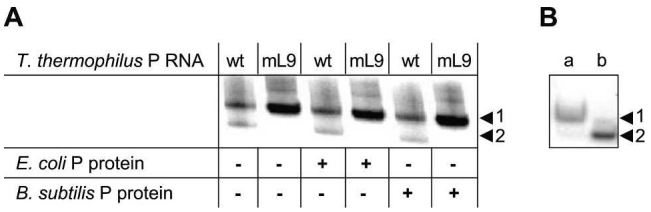

FIGURE 2. (*A*) Native PAGE analysis of *T. thermophilus* P RNA and its L9 mutant in the presence (+) or absence (−) of P protein. Trace amounts (≤50 fmol) of 3′-end labeled P RNA were incubated in buffer KN4.5 for 5 min at 55°C followed by 50 min at 37°C, and either with our without the addition of 40 nM RNase P protein for another 15 min at 37°C. Samples were loaded and run on 11.25% polyacrylamide gels in 1× THE buffer supplemented with 100 mM NH_4OAc and 4.5 mM $MgCl_2$ (for further details, see Materials and Methods). (*B*) Stability of *T. thermophilus* wt P RNA conformers studied by reelectrophoresis after elution. *T. thermophilus* wt P RNA (10 nmol including 3′-end labeled P RNA) was preincubated (see Materials and Methods) and then loaded on a native 11.25% polyacrylamide gel as in *A*. The two conformers (bands *1*,*2*) were then eluted separately at 4°C, and aliquots of each band were loaded onto another native 11.25% polyacrylamide gel. Electrophoreses were performed at ≤15°C. Under these conditions, with the temperature not exceeding 15°C during elution and reelectrophoresis, both conformers did not reequilibrate to a substantial extent.

Compared to the *E. coli* wild type (wt), ribozyme activity of this hybrid P RNA at 37°C was also essentially unchanged, but relatively increased to a substantial extent at 55°C (Fig. 3C; Table 1). Again the mutant P RNA was functional in vivo (Table 3). Finally, an exceptional kind of P1–P9 interaction exists in some P RNAs of the genus *Mycoplasma*, which possess a P RNA of type B and where P9 and P1 juxtapose via a pseudoknot instead of the tetraloop–helix contact apparent in many type A P RNAs (Massire et al. 1997). Built into *E. coli* P RNA as an interaction module expected to be of particularly high stability (Fig. 3B, *E. coli* P1P9 *Mgen*), the pseudoknot of *M. genitalium* had little effect on the RNA-alone reaction at 37°C but substantially increased the cleavage rate at 55°C (Fig. 3C), the maximum cleavage rate obtained with this variant even exceeding that of *E. coli* P1P9 *Tth* (Table 1). In the holoenzyme reaction, cleavage rates were roughly twice that of *E. coli* wt P RNA (Table 2), and again, the hybrid P RNA was fully functional in vivo (Table 3). Finally, we intended to stabilize the interacting module even further by an A117 to C mutation in *Mgen* P9 to introduce an additional Watson–Crick base pair (Fig. 3B). This mutation generated a variant with the highest maximum turnover rate at 55°C yet described for a P RNA ribozyme (Table 1).

The fast substrate turnover catalyzed by the chimeric RNAs *E. coli* P1P9 *Mgen* and *MgenA117C* in the RNA-alone reaction at 55°C was associated with an increase in the single turnover $K_{m(sto)}$ compared with cleavage at 37°C, in particular for variant *E. coli* P1P9 *MgenA117C* (Table 1). This effect may be due to a loss in substrate binding affinity or to a reduction in the fraction of P RNAs that are competent to bind the substrate at 55°C. While this K_m effect may have various reasons, the stronger K_m effect for variant *E. coli* P1P9 *MgenA117C* (Fig. 3B) may be explained by the mutant C117–G108 bp constraining the orientation of A118, such that stacking of A118 on another bulged A residue in P11 (A233) (Fig. 3A; Lescoute and Westhof 2006) is weakened and becomes unstable at the higher temperature of 55°C.

CONCLUSIONS

From the presented data we conclude that the P1–L9 tertiary contact is crucial for folding and activity of P RNA from the thermophile *T. thermophilus* at high temperatures and low magnesium ion concentrations, conditions that require high intrinsic stability of the RNA. Our native PAGE analysis suggests that this interacting module represents one of the key anchoring points toward folding into the most active RNA conformer. These results extend present knowledge on the thermostability of P RNA from *T. thermophilus*: While Pan and coworkers identified 12 key base identities in the *T. thermophilus* S-domain that explain its stability increase over the corresponding *E. coli* domain (Baird et al. 2006), we were able to pinpoint an interdomain strut crucial for function of the entire RNA.

In contrast, the P1–L9 interaction appears degenerate in *E. coli*-like mesophilic P RNAs and could be completely disrupted without compromising function in vitro as well as in vivo. Yet, though not made use of in *E. coli*, in this P RNA the location of the P1–L9 interaction module has nonetheless remained a key position for placing an architecturally highly effective interdomain strut: If building in a strongly interacting P1–L9 module, *E. coli* P RNA gains substantially in activity at high temperatures. The architectural framework governing P RNA overall statics has thus been preserved between the thermophilic and mesophilic P RNA.

Finally, our findings identify the P1–L9 receptor/tetraloop of *T. thermophilus* and the corresponding pseudoknot from *M. genitalium* as (thermo)stabilization modules for complex RNAs that comply with the concept of modular "plug and play" interchangeability (Costa and Michel 1995, 1997; Qin et al. 2001). They may thus expand the spectrum of modules that can be exploited to stabilize larger RNAs for structural analysis (Ferré-D'Amaré et al. 1998).

MATERIALS AND METHODS

Cloning of transcription templates and complementation plasmids

All plasmids were constructed by standard PCR and cloning techniques.

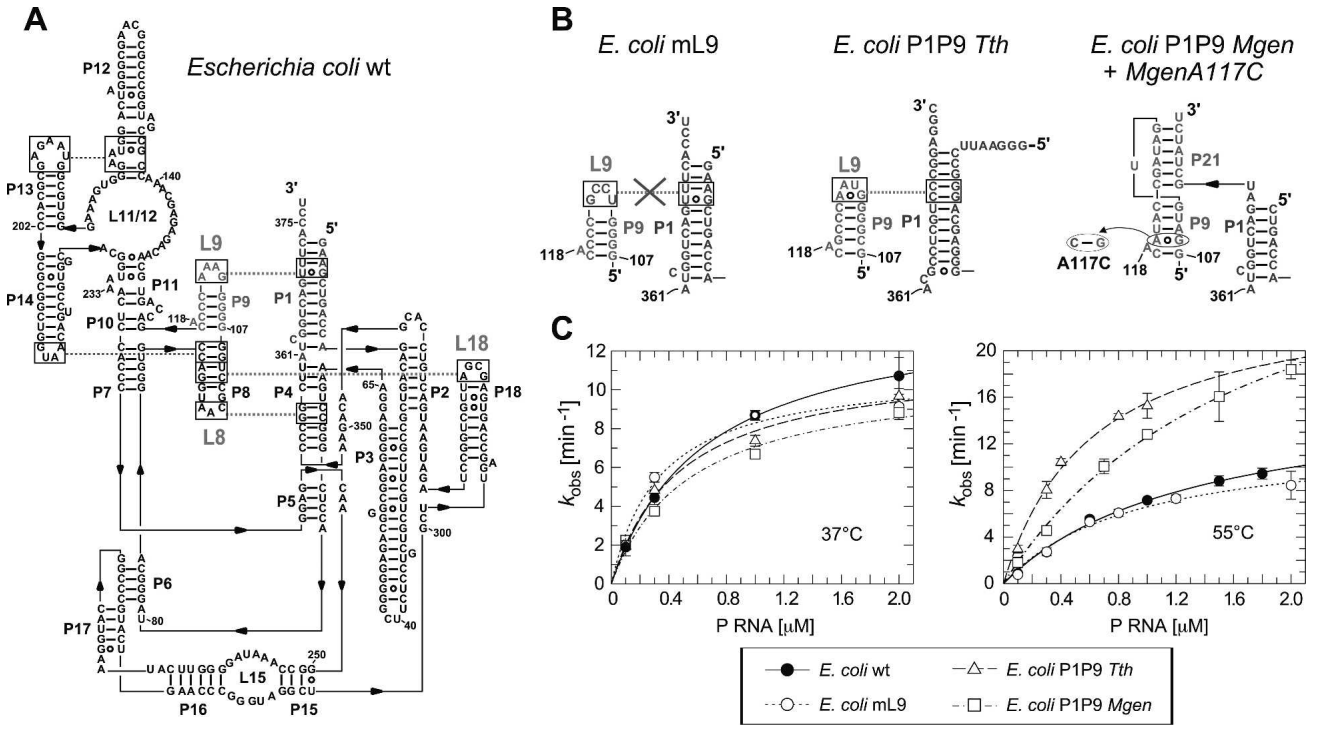

FIGURE 3. Secondary structure presentation of (*A*) *E. coli* wild-type (wt) P RNA and (*B*) alterations in the P1–P9 mutants thereof. mL9: Nucleotide changes in loop L9 that disrupt the P1–L9 interaction; P1P9 *Tth*: *E. coli* P1P9 replaced with the corresponding elements of *T. thermophilus* P RNA; P1P9 *Mgen*: *E. coli* P1P9 replaced with the pseudoknot from *M. genitalium*; P1P9 *MgenA117C*: variant of P1P9 *Mgen*, with a single nucleotide (A117C) exchanged. (*C*) Processing assays with the *E. coli* P RNA variants performed as described in the legend to Figure 1C.

Preparation and labeling of substrate and P RNA

ptRNA substrate and P RNAs were obtained by run-off transcription with recombinant bacteriophage T7 RNA polymerase and were 5′- and 3′-end labeling essentially as described (Heide et al. 1999; Busch et al. 2000). The *T. thermophilus* ptRNA^{Gly} substrate was transcribed from plasmid pSBpt3′HH linearized with BamHI (Busch et al. 2000); *E. coli* wild-type P RNA was transcribed from plasmid pJA2′ linearized with FokI (Vioque et al. 1988; Busch et al. 2000), *T. thermophilus* P RNA variants from plasmid pUC19*TthrnpB*wt and pUC19*TthrnpB*mL9 linearized with EheI; all *E. coli* mutant P RNAs were transcribed from respective pUC19-derivatives linearized with EcoRI (*E. coli* mL9, *E. coli* P1P9 *Tth*, *E. coli* P1P9 *Mgen*, and *E. coli* P1P9 *MgenA117C*). The gift of pUC19*TthrnpB*wt from Andreas Werner, group of Eric Westhof, IBMC Strasbourg, is gratefully acknowledged.

RNase P RNA and holoenzyme activity assays

RNase P RNA-alone activity assays were performed in 100 mM $Mg(OAc)_2$, 100 mM NH_4OAc, 50 mM MES, and 2 mM EDTA (pH 6.0), with trace amounts of 5′-end labeled substrate and P RNA concentrations in the range of 0.1–3 μM. Before starting the reaction, substrate and P RNA were preincubated separately in the assay buffer (ptRNA^{Gly} substrate for 5 min at 55°C and 20 min at 37°C, P RNAs for 5 min at 55°C and 55 min at 37°C). Reactions were run for 5–30 min at 37°C or 55°C as indicated. Activity of RNase P holoenzymes was measured in buffer KN (20 mM HEPES, 150 mM NH_4OAc, 2 mM spermidine, 0.05 mM spermine, 4 mM β-mercaptoethanol at pH 7.4 at 37°C) containing 2 or 4.5 mM $Mg(OAc)_2$ (buffer KN2 and KN4.5; Wegscheid and Hartmann 2006), at concentrations of 10 nM P RNA, 100 nM substrate, and 40 nM P protein (recombinantly expressed and purified exactly as in Marszalkowski et al. 2006). Prior to the reaction, substrate and P RNA were preincubated in the reaction buffer (substrate as above, P RNA for 5 min at 55°C and 50 min at 37°C); P protein was then added to the P RNA and preincubation continued for another 5 min at 37°C, after which substrate was added. Analysis of cleavage reactions and data evaluation were carried out as described (Busch et al. 2000).

Folding analysis by native PAGE

Folding analyses were performed essentially as described (Wegscheid and Hartmann 2006). In Figure 2A, trace amounts (≤50 fmol) of 3′-end labeled P RNA were incubated in buffer KN4.5 (see above) for 5 min at 55°C followed by 50 min at 37°C and either with or without the addition of 40 nM RNase P protein for another 15 min at 37°C. After addition of an equal volume of loading buffer (10% [v/v] glycerol, 4.5 mM $MgCl_2$, 0.025% [w/v] each bromophenol blue and xylene cyanol), samples were run on an 11.25% (v/v) polyacrylamide gel containing 66 mM HEPES, 33 mM Tris, 0.1 mM EDTA, 100 mM NH_4OAc, and 4.5 mM $Mg(OAc)_2$ (pH 7.4) (buffer system

TABLE 3. In vivo complementation screen in *E. coli rnpB* mutant strain BW

	Complementation	
rnpB	37°	43°
None	–	–
E. coli wt	++	++
E. coli C293 or C292	–	–
E. coli mL9	++	++
E. coli P1P9 *Tth*	++	++
E. coli P1P9 *Mgen*	++	++
E. coli P1P9 *MgenA117C*	+	++
T. thermophilus wt	–	–
T. thermophilus mL9	n.d.	n.d.

Growth of cells was monitored in the presence of 0.5% (w/v) glucose (without arabinose), conditions under which the chromosomal *rnpB* gene of the *E. coli* mutant strain BW is not expressed (at 37° as well as 43°C); cells were transformed with derivatives of the low copy plasmid pACYC177 that contained *rnpB* genes coding for P RNAs and mutants thereof under control of the native *rnpB* promoter. *E. coli rnpB* genes with G293C or G292C point mutations were previously shown to be lethal (Wegscheid and Hartmann 2006); (–) No cell growth; (++) growth with equal numbers of colonies on arabinose and glucose plates; (+) somewhat decreased complementation efficiency according to number and size of colonies; (n.d.) not determined because the *T. thermophilus* wild-type (wt) *rnpB* gene already does not complement, likely because of folding traps (data not shown) at the growth temperatures of the *E. coli* strain.

adapted from Buck et al. 2005), with the gel temperature not exceeding 15°C. RNA bands were visualized with a Bio-Imaging Analyzer (FLA 3000-2R, Fujifilm). For reelectrophoresis and activity testing of *T. thermophilus* wt P RNA conformers (Fig. 2B), 20 nM of unlabeled P RNA plus 20×10^3 Cerenkov cpm of 3′-end labeled P RNA per gel lane were preincubated in buffer KN4.5 for 10 min at 55°C in a volume of 7 μL; after addition of 7 μL loading buffer (see above), samples were subjected to native PAGE as described above. After electrophoresis and 1 h of phosphorimager plate exposition, the two conformers were excised separately from the gel and eluted in 50 μL of buffer KN4.5 (see above) without Mg^{2+} by shaking overnight at 4°C. To analyze stability of the conformers, eluted material from each band was subsequently supplemented with loading buffer and run on a second native polyacrylamide gel (Fig. 2B). To compare the conformers for differences in catalytic activity, ~3.5 nM of each eluted conformer were used in holoenzyme cleavage assays performed under multiple turnover conditions (reaction buffer KN4.5, 100 nM ptRNA, 40 nM *B. subtilis* RNase P protein). Assays were carried out at 22°C without any preincubation steps to eliminate potential heat-induced conformational changes.

In vivo complementation assays in *E. coli* strain BW

In vivo complementation assays were performed in the *E. coli rnpB* mutant strain BW with derivatives of the low copy plasmid pACYC177 precisely as described (Wegscheid and Hartmann 2006).

ACKNOWLEDGMENTS

This work was supported by the Deutsche Forschungsgemeinschaft and the Fonds der Chemischen Industrie.

Received August 2, 2007; accepted September 10, 2007.

REFERENCES

Baird, N.J., Srividya, N., Krasilnikov, A.S., Mondragon, A., Sosnick, T.R., and Pan, T. 2006. Structural basis for altering the stability of homologous RNAs from a mesophilic and a thermophilic bacterium. *RNA* **12:** 598–606.

Brown, J.W., Nolan, J.M., Haas, E.S., Rubio, M.A., Major, F., and Pace, N.R. 1996. Comparative analysis of ribonuclease P RNA using gene sequences from natural microbial populations reveals tertiary structural elements. *Proc. Natl. Acad. Sci.* **93:** 3001–3006.

Buck, A.H., Dalby, A.B., Poole, A.W., Kazantsev, A.V., and Pace, N.R. 2005. Protein activation of a ribozyme: The role of bacterial RNase P protein. *EMBO J.* **24:** 3360–3368.

Busch, S., Kirsebom, L.A., Notbohm, H., and Hartmann, R.K. 2000. Differential role of the intermolecular base-pairs G292-C75 and G293-C74 in the reaction catalyzed by *Escherichia coli* RNase P RNA. *J. Mol. Biol.* **299:** 941–951.

Costa, M. and Michel, F. 1995. Frequent use of the same tertiary motif by self-folding RNAs. *EMBO J.* **14:** 1276–1285.

Costa, M. and Michel, F. 1997. Rules for RNA recognition of GNRA tetraloops deduced by in vitro selection: Comparison with in vivo evolution. *EMBO J.* **16:** 3289–3302.

Darr, S.C., Zito, K., Smith, D., and Pace, N.R. 1992. Contributions of phylogenetically variable structural elements to the function of the ribozyme ribonuclease P. *Biochemistry* **31:** 328–333.

Ferré-D'Amaré, A.R., Zhou, K., and Doudna, J.A. 1998. A general module for RNA crystallization. *J. Mol. Biol.* **279:** 621–631.

Gößringer, M., Kretschmer-Kazemi Far, R., and Hartmann, R.K. 2006. Analysis of RNase P protein (*rnpA*) expression in *Bacillus subtilis* utilizing strains with suppressible *rnpA* expression. *J. Bacteriol.* **188:** 6816–6823.

Guerrier-Takada, C., Gardiner, K., Marsh, T., Pace, N., and Altman, S. 1983. The RNA moiety of ribonuclease P is the catalytic subunit of the enzyme. *Cell* **35:** 849–857.

Hall, T.A. and Brown, J.W. 2001. The ribonuclease P family. *Methods Enzymol.* **341:** 56–77.

Hartmann, R.K. and Erdmann, V.A. 1991. Analysis of the gene encoding the RNA subunit of ribonuclease P from *T. thermophilus* HB8. *Nucleic Acids Res.* **19:** 5957–5964. doi: 10.1093/nar/19.21.5957.

Heide, C., Pfeiffer, T., Nolan, J.M., and Hartmann, R.K. 1999. Guanosine 2-NH_2 groups of *Escherichia coli* RNase P RNA involved in intramolecular tertiary contacts and direct interactions with tRNA. *RNA* **5:** 102–116.

Lescoute, A. and Westhof, E. 2006. The interaction networks of structured RNAs. *Nucleic Acids Res.* **34:** 6587–6604. doi: 10.1093/nar/gkl963.

Loria, A. and Pan, T. 1996. Domain structure of the ribozyme from eubacterial ribonuclease P. *RNA* **2:** 551–563.

Loria, A. and Pan, T. 1997. Recognition of the T stem–loop of a pre-tRNA substrate by the ribozyme from *Bacillus subtilis* ribonuclease P. *Biochemistry* **36:** 6317–6325.

Marszalkowski, M., Teune, J.H., Steger, G., Hartmann, R.K., and Willkomm, D.K. 2006. Thermostable RNase P RNAs lacking P18 identified in the *Aquificales*. *RNA* **12:** 1915–1921.

Massire, C., Jaeger, L., and Westhof, E. 1997. Phylogenetic evidence for a new tertiary interaction in bacterial RNase P RNAs. *RNA* **3:** 553–556.

Massire, C., Jaeger, L., and Westhof, E. 1998. Derivation of the three-dimensional architecture of bacterial ribonuclease

P RNAs from comparative sequence analysis. *J. Mol. Biol.* **279:** 773–793.

Pomeranz Krummel, D.A. and Altman, S. 1999. Verification of phylogenetic predictions in vivo and the importance of the tetraloop motif in a catalytic RNA. *Proc. Natl. Acad. Sci.* **96:** 11200–11205.

Qin, H., Sosnick, T.R., and Pan, T. 2001. Modular construction of a tertiary RNA structure: The specificity domain of the *Bacillus subtilis* RNase P RNA. *Biochemistry* **40:** 11202–11210.

Schedl, P., Primakoff, P., and Roberts, J. 1974. Processing of *E. coli* tRNA precursors. *Brookhaven Symp. Biol.* **26:** 53–76.

Schön, A. 1999. Ribonuclease P: The diversity of a ubiquitous RNA processing enzyme. *FEMS Microbiol. Rev.* **23:** 391–406.

Torres-Larios, A., Swinger, K.K., Krasilnikov, A.S., Pan, T., and Mondragon, A. 2005. Crystal structure of the RNA component of bacterial ribonuclease P. *Nature* **437:** 584–587.

Vioque, A., Arnez, J., and Altman, S. 1988. Protein–RNA interactions in the RNase P holoenzyme from *Escherichia coli*. *J. Mol. Biol.* **202:** 835–848.

Wegscheid, B. and Hartmann, R.K. 2006. The precursor tRNA 3′-CCA interaction with *Escherichia coli* RNase P RNA is essential for catalysis by RNase P in vivo. *RNA* **12:** 2135–2148.